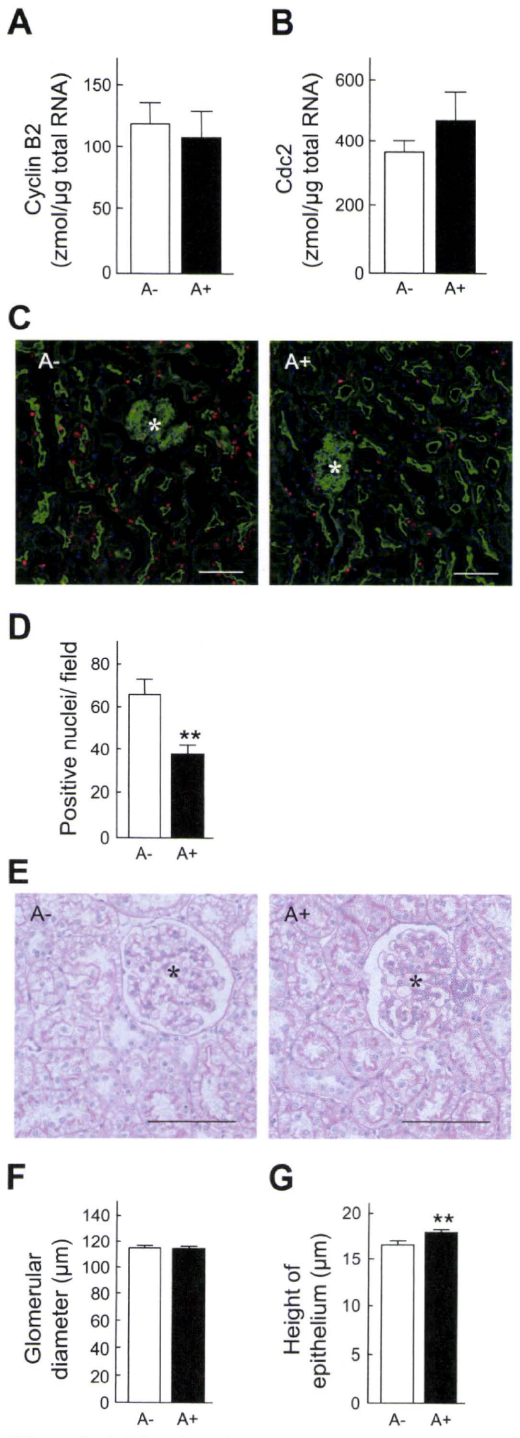

Fig. 7. Effects of administration of 2-cyanoethyl alsterpaullone (CE-ALP) in Nx rats. Nx rats were subcutaneously treated with vehicle (A−) or CE-ALP (A+, 0.5 mg/kg) for 14 days immediately after Nx. *A* and *B*: measurement of mRNA levels of Cyclin B2 (*A*) and Cdc2 (*B*) by real-time PCR. *C*: immunofluorescent analysis of Ki-67. *D*: numbers of stained nuclei in the proximal tubules were counted in 6 independent regions at 100-fold magnification. *E*: representative photographs of PAS staining of the remnant kidney. *F* and *G*: measurement of glomerular diameter (*F*) and height of epithelial cells (*G*). *, Glomeruli. Scale bars 100 μm. $^{**}P < 0.01$, significantly different from vehicle-treated (A−) rats.

hypertrophy in unilaterally nephrectomized mice by modulating RNA and protein synthesis (3). Most recently, it was demonstrated that S6 kinase 1 (S6K1), a downstream effector of mTOR, plays a major role in the development of compensatory renal hypertrophy in the same model using S6K1-knockout mice (4). Thus the molecular mechanisms of renal hypertrophy on the mTOR signaling pathway have been elucidated in detail. In this study, the increased expression in Cyclin B2 and Cdc2 was completely abolished, and the signals for Ki-67 and p-histone H3 in the epithelial cells were clearly decreased by treatment with everolimus in the Nx rats (Figs. 6 and 8). Therefore it can be inferred that everolimus inhibited both cellular hypertrophy and hyperplasia by modulating RNA and protein synthesis and enhanced cell division arrest by reducing the levels of Cyclin B-Cdc2, resulting in severe renal damage in compensative CRF.

Because the mTOR pathway affects both hypertrophy and hyperplasia, it is difficult to evaluate the specific contribution of the upregulation of Cyclin B-Cdc2 to the epithelial proliferation. Treatment with CE-ALP, a specific inhibitor of Cyclin B-Cdc2 with an IC_{50} value of 0.23 nM (19), resulted in further deterioration of renal function, as indicated by the significant increase of BUN, the moderate increase in PCr and albuminuria, and the decreased CCr (Table 3). Moreover, the proliferation of epithelial cells in CE-ALP-treated rats assessed by Ki-67-positive nuclei as well as immunohistochemistry of p-histone H3 was decreased to 50–60% of that of vehicle-treated rats (Figs. 7 and 8). These results indicated that the enhanced expression of Cyclin B2-Cdc2 actually acted as an M-phase regulator to retain the renal tubular function in rat kidney. On the other hand, the height of epithelial cells was significantly increased by the treatment with CE-ALP (Fig. 7*G*). Two recent studies revealed that cell cycle polarity protein kinase, which is an upstream molecule of Cdc2, serves as a sensor for cellular length to regulate mitotic entry in the fission yeast (25, 28). Although further investigation of a precise molecular mechanism is required in mammalian cells, the inhibition of Cdc2 by CE-ALP in the compensative period might associate with the growth of epithelium size in proximal tubules.

In the present study, molecular events specific to the renal proximal tubules have been clearly observed in Nx rats with CRF progression. On the basis of these transcriptome data and subsequent examinations, Cyclin B2-Cdc2 was revealed to be important to the proliferative response of proximal tubular cells in the compensated kidney. Therefore, the present results advance the knowledge of the contribution of cell cycle regulators to pathophysiology of tubular restoration and/or degeneration in progressive CRF. The hypothesized molecular mechanisms of proliferation inhibitors and proximal tubular hyperplasia and hypertrophy in CRF are summarized in Fig. 9. In the normal kidney, a portion of epithelial cells in the proximal tubules was positive for Cyclin B-Cdc2 (Fig. 9*B*). After renal ablation, hyperplasia via the induction of the M-phase regulator Cyclin B-Cdc2 and hypertrophy occur simultaneously in an attempt to recover the reduction in nephron mass in early-stage CRF (Fig. 9*C*). However, in end-stage CRF, the enhancement of Cyclin B-Cdc2 was reduced. The remnant viable tubules may lose the ability to regenerate new cells at the fibrotic stage, and thus further tubular atrophy and degeneration occur (Fig. 9*D*). The severe renal deterioration caused by treatment with the mTOR inhibitor might be mediated by inhibition of both

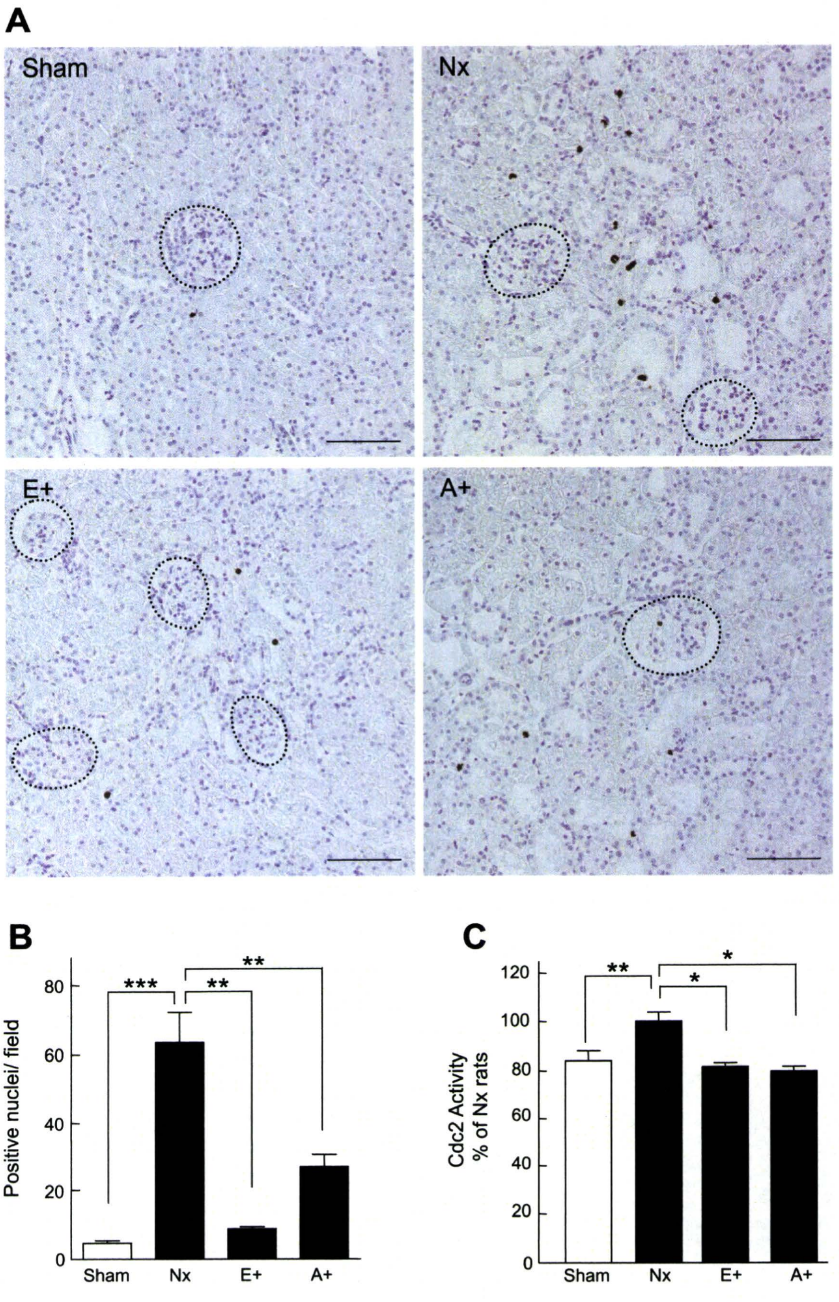

Fig. 8. Effects of everolimus and CE-ALP on expression of phospho (p)-histone H3 and activities of Cdc2 in the kidney. *A*: representative photograph of kidney stained with p-histone H3 in sham-operated rats, Nx rats, and Nx rats treated with everolimus (E+) or CE-ALP (A+) at 2 wk after surgery. Dotted circles, glomeruli. Scale bars 100 μm. *B*: numbers of nuclei stained for p-histone H3 in the proximal tubules were counted at 100-fold magnification. *C*: activities of Cdc2 after administration of everolimus and CE-ALP. Multiple comparisons were performed with Bonferroni's test after a 1-way ANOVA. $*P < 0.05$, $**P < 0.01$, $***P < 0.001$, significantly different.

hyperplasia and hypertrophy because the mTOR pathway affects various factors involved in the cell cycle, RNA modulation, and protein synthesis (Fig. 9*E*). Administration of a specific inhibitor for Cdc2 selectively inhibited hyperplasia of epithelial cells, resulting in a moderate reduction in renal function (Fig. 9*F*).

Considering the time-dependent changes in the gene expression profile of Cyclin B2 and Cdc2 after Nx and the balance between tubular hyperplasia and hypertrophy, the temporal induction of Cyclin B2 and Cdc2 was suggested to be a marker and one of the crucial mechanisms for proliferating proximal tubular cells in early-stage CRF. If we can discover another specific inhibitor of hypertrophy without effects on Cyclin B-Cdc2, it may be a potential regenerative agent that accelerates compensative hyperplasia in the early stage of ablation of nephron mass.

GRANTS

This work was supported in part by a grant-in-aid for Research on Biological Markers for New Drug Development and Health and Labour Sciences Research Grants from the Ministry of Health, Labour and Welfare of Japan (08062855 to S. Masuda); by the Japan Health Science Foundation "Research on Health Sciences Focusing on Drug Innovation" (KH23303 to S. Masuda); and by a Grant-in-Aid for Scientific Research (A) (20249036 to K. Inui), a Grant-in-Aid for Young Scientists (A) (21689017 to S. Masuda), and a Grant-in-Aid for Japan Society for the Promotion of Science (JSPS) Fellows (20-2438 to K. Nishihara) from the Ministry of Education, Science, Culture,

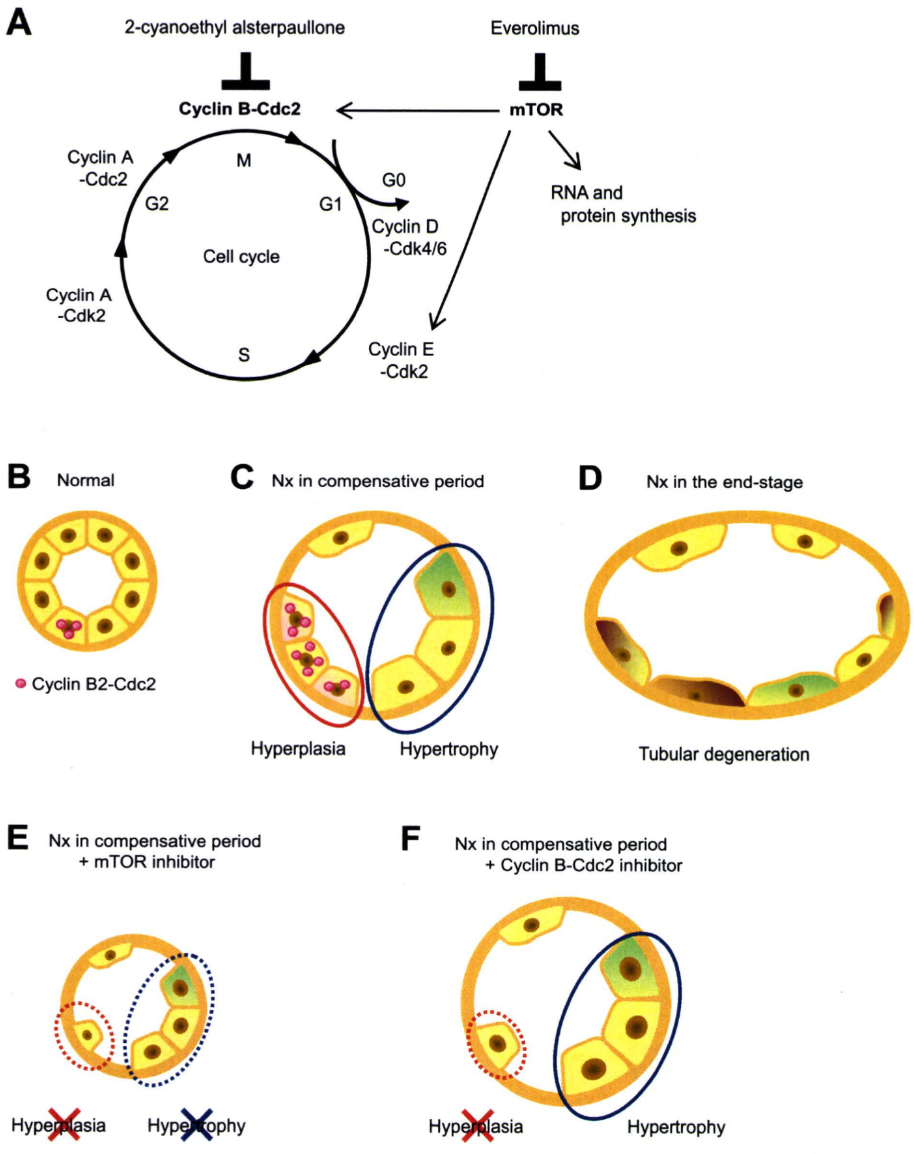

Fig. 9. The hypothesized scheme of molecular responses in tubular epithelial hyperplasia and hypertrophy in chronic renal failure (CRF). *A*: molecular targets of mammalian target of rapamycin (mTOR) inhibitor and Cdc2 inhibitor in the cell cycle and mTOR pathway. *B–F*: renal proximal tubules of normal rats (*B*) and Nx rats (*C–F*). A portion of the renal epithelial cells in the proximal tubules was positive for Cyclin B2-Cdc2 (*B*). Hyperplasia via induction of Cyclin B2-Cdc2, G_2-M cyclins, and hypertrophy simultaneously occurred in the compensative period in CRF rats (*C*). In end-stage CRF, tubular atrophy and degeneration were observed (*D*). *E*: proximal tubules treated with the mTOR inhibitor. Neither hyperplasia nor hypertrophy of tubular epithelial cells occurred, resulting in severe renal damage. *F*: proximal tubules treated with the Cyclin B-Cdc2 inhibitor. Only hyperplasia was inhibited, and a moderate reduction in renal function was observed.

Sports and Technology of Japan (MEXT). K. Nishihara is a Research Fellow of the JSPS.

DISCLOSURES

No conflicts of interest are declared by the authors.

REFERENCES

1. **Bonventre JV.** Dedifferentiation and proliferation of surviving epithelial cells in acute renal failure. *J Am Soc Nephrol* 14, *Suppl* 1: S55–S61, 2003.
2. **Bottinger EP, Bitzer M.** TGF-beta signaling in renal disease. *J Am Soc Nephrol* 13: 2600–2610, 2002.
3. **Chen JK, Chen J, Neilson EG, Harris RC.** Role of mammalian target of rapamycin signaling in compensatory renal hypertrophy. *J Am Soc Nephrol* 16: 1384–1391, 2005.
4. **Chen JK, Chen J, Thomas G, Kozma SC, Harris RC.** S6 kinase 1 knockout inhibits uninephrectomy- or diabetes-induced renal hypertrophy. *Am J Physiol Renal Physiol* 297: F585–F593, 2009.
5. **Frazier KS, Paredes A, Dube P, Styer E.** Connective tissue growth factor expression in the rat remnant kidney model and association with tubular epithelial cells undergoing transdifferentiation. *Vet Pathol* 37: 328–335, 2000.
6. **Fung TK, Poon RYC.** A roller coaster ride with the mitotic cyclins. *Semin Cell Dev Biol* 16: 335–342, 2005.
7. **Fushimi K, Uchida S, Hara Y, Hirata Y, Marumo F, Sasaki S.** Cloning and expression of apical membrane water channel of rat kidney collecting tubule. *Nature* 361: 549–552, 1993.
8. **Gamba G, Miyanoshita A, Lombardi M, Lytton J, Lee WS, Hediger MA, Hebert SC.** Molecular cloning, primary structure, and characterization of two members of the mammalian electroneutral sodium-(potassium)-chloride cotransporter family expressed in kidney. *J Biol Chem* 269: 17713–17722, 1994.
9. **Gerdes J, Lemke H, Baisch H, Wacker HH, Schwab U, Stein H.** Cell cycle analysis of a cell proliferation-associated human nuclear antigen defined by the monoclonal antibody Ki-67. *J Immunol* 133: 1710–1715, 1984.
10. **Harper JV, Brooks G.** The mammalian cell cycle: an overview. *Methods Mol Biol* 296: 113–153, 2005.
11. **Hayslett JP.** Functional adaptation to reduction in renal mass. *Physiol Rev* 59: 137–164, 1979.
12. **Hendzel MJ, Wei Y, Mancini MA, Van Hooser A, Ranalli T, Brinkley BR, Bazett-Jones DP, Allis CD.** Mitosis-specific phosphorylation of

histone H3 initiates primarily within pericentromeric heterochromatin during G2 and spreads in an ordered fashion coincident with mitotic chromosome condensation. *Chromosoma* 106: 348–360, 1997.

13. **Hori R, Okumura K, Kamiya A, Nihira H, Nakano H.** Ampicillin and cephalexin in renal insufficiency. *Clin Pharmacol Ther* 34: 792–798, 1983.
14. **Horiba N, Masuda S, Takeuchi A, Saito H, Okuda M, Inui K.** Gene expression variance based on random sequencing in rat remnant kidney. *Kidney Int* 66: 29–45, 2004.
15. **Hostetter TH, Olson JL, Rennke HG, Venkatachalam MA, Brenner BM.** Hyperfiltration in remnant nephrons: a potentially adverse response to renal ablation. *Am J Physiol Renal Fluid Electrolyte Physiol* 241: F85–F93, 1981.
16. **Jackman M, Firth M, Pines J.** Human cyclins B1 and B2 are localized to strikingly different structures: B1 to microtubules, B2 primarily to the Golgi apparatus. *EMBO J* 14: 1646–1654, 1995.
17. **Ji L, Masuda S, Saito H, Inui K.** Down-regulation of rat organic cation transporter rOCT2 by 5/6 nephrectomy. *Kidney Int* 62: 514–524, 2002.
18. **Kawachi H, Koike H, Kurihara H, Sakai T, Shimizu F.** Cloning of rat homologue of podocin: expression in proteinuric states and in developing glomeruli. *J Am Soc Nephrol* 13: 46–56, 2003.
19. **Kunick C, Zeng Z, Gussio R, Zaharevitz D, Leost M, Totzke F, Schachtele C, Kubbutat MH, Meijer L, Lemcke T.** Structure-aided optimization of kinase inhibitors derived from alsterpaullone. *Chembiochem* 6: 541–549, 2005.
20. **Kwon TH, Frokiaer J, Knepper MA, Nielsen S.** Reduced AQP1, -2, and -3 levels in kidneys of rats with CRF induced by surgical reduction in renal mass. *Am J Physiol Renal Physiol* 275: F724–F741, 1998.
21. **Lee CH, Inoki K, Guan KL.** mTOR pathway as a target in tissue hypertrophy. *Annu Rev Pharmacol Toxicol* 47: 443–467, 2007.
22. **Leonard MO, Cottell DC, Godson C, Brady HR, Taylor CT.** The role of HIF-1alpha in transcriptional regulation of the proximal tubular epithelial cell response to hypoxia. *J Biol Chem* 278: 40296–40304, 2003.
23. **Liu B, Preisig PA.** Compensatory renal hypertrophy is mediated by a cell cycle-dependent mechanism. *Kidney Int* 62: 1650–1658, 2002.
24. **Lloberas N, Cruzado JM, Franquesa M, Herrero-Fresneda I, Torras J, Alperovich G, Rama I, Vidal A, Grinyo JM.** Mammalian target of rapamycin pathway blockade slows progression of diabetic kidney disease in rats. *J Am Soc Nephrol* 17: 1395–1404, 2006.
25. **Martin SG, Berthelot-Grosjean M.** Polar gradients of the DYRK-family kinase Pom1 couple cell length with the cell cycle. *Nature* 459: 852–856, 2009.
26. **Masuda S, Saito H, Nonoguchi H, Tomita K, Inui K.** mRNA distribution and membrane localization of the OAT-K1 organic anion transporter in rat renal tubules. *FEBS Lett* 407: 127–131, 1997.
27. **Megyesi J, Price PM, Tamayo E, Safirstein RL.** The lack of a functional $p21^{WAF1/CIP1}$ gene ameliorates progression to chronic renal failure. *Proc Natl Acad Sci USA* 96: 10830–10835, 1999.
28. **Moseley JB, Mayeux A, Paoletti A, Nurse P.** A spatial gradient coordinates cell size and mitotic entry in fission yeast. *Nature* 459: 857–860, 2009.
29. **Nakagawa S, Masuda S, Nishihara K, Inui K.** mTOR inhibitor everolimus ameliorates progressive tubular dysfunction in chronic renal failure rats. *Biochem Pharmacol* 79: 67–76, 2010.
30. **Nishihara K, Masuda S, Ji L, Katsura T, Inui K.** Pharmacokinetic significance of luminal multidrug and toxin extrusion 1 in chronic renal failure rats. *Biochem Pharmacol* 73: 1482–1490, 2007.
31. **Price PM, Safirstein RL, Megyesi J.** The cell cycle and acute kidney injury. *Kidney Int* 76: 604–613, 2009.
32. **Satyanarayana A, Kaldis P.** Mammalian cell-cycle regulation: several Cdks, numerous cyclins and diverse compensatory mechanisms. *Oncogene* 28: 2925–2939, 2009.
33. **Shankland SJ, Wolf G.** Cell cycle regulatory proteins in renal disease: role in hypertrophy, proliferation, and apoptosis. *Am J Physiol Renal Physiol* 278: F515–F529, 2000.
34. **Shillingford JM, Murcia NS, Larson CH, Low SH, Hedgepeth R, Brown N, Flask CA, Novick AC, Goldfarb DA, Kramer-Zucker A, Walz G, Piontek KB, Germino GG, Weimbs T.** The mTOR pathway is regulated by polycystin-1, and its inhibition reverses renal cystogenesis in polycystic kidney disease. *Proc Natl Acad Sci USA* 103: 5466–5471, 2006.
35. **Shimamura T, Morrison AB.** A progressive glomerulosclerosis occurring in partial five-sixths nephrectomized rats. *Am J Pathol* 79: 95–106, 1975.
36. **Suzuki H, Inoue T, Matsushita T, Kobayashi K, Horii I, Hirabayashi Y, Inoue T.** In vitro gene expression analysis of nephrotoxic drugs in rat primary renal cortical tubular cells. *J Appl Toxicol* 28: 237–248, 2008.
37. **Taal MW, Zandi-Nejad K, Weening B, Shahsafaei A, Kato S, Lee KW, Ziai F, Jiang T, Brenner BM, MacKenzie HS.** Proinflammatory gene expression and macrophage recruitment in the rat remnant kidney. *Kidney Int* 58: 1664–1676, 2000.
38. **Takeuchi A, Masuda S, Saito H, Doi T, Inui K.** Role of kidney-specific organic anion transporters in the urinary excretion of methotrexate. *Kidney Int* 60: 1058–1068, 2001.
39. **Tao Y, Kim J, Schrier RW, Edelstein CL.** Rapamycin markedly slows disease progression in a rat model of polycystic kidney disease. *J Am Soc Nephrol* 16: 46–51, 2005.
40. **Tsuji M, Monkawa T, Yoshino J, Asai M, Fukuda S, Kawachi H, Shimizu F, Hayashi M, Saruta T.** Microarray analysis of a reversible model and an irreversible model of anti-Thy-1 nephritis. *Kidney Int* 69: 996–1004, 2006.
41. **Weiland C, Ahr HJ, Vohr HW, Ellinger-Ziegelbauer H.** Characterization of primary rat proximal tubular cells by gene expression analysis. *Toxicol In Vitro* 21: 466–491, 2007.
42. **Wolf G, Stahl RA.** Angiotensin II-stimulated hypertrophy of LLC-PK1 cells depends on the induction of the cyclin-dependent kinase inhibitor $p27^{Kip1}$. *Kidney Int* 50: 2112–2119, 1996.
43. **Xiong Y, Hannon GJ, Zhang H, Casso D, Kobayashi R, Beach D.** p21 is a universal inhibitor of cyclin kinases. *Nature* 366: 701–704, 1993.
44. **Yamada M, Katsuma S, Adachi T, Hirasawa A, Shiojima S, Kadowaki T, Okuno Y, Koshimizu T, Fujii S, Sekiya Y, Miyamoto Y, Tamura M, Yumura W, Nihei H, Kobayashi M, Tsujimoto G.** Inhibition of protein kinase CK2 prevents the progression of glomerulonephritis. *Proc Natl Acad Sci USA* 102: 7736–7741, 2005.
45. **Yang Y, Wang J, Qin L, Shou Z, Zhao J, Wang H, Chen Y, Chen J.** Rapamycin prevents early steps of the development of diabetic nephropathy in rats. *Am J Nephrol* 27: 495–502, 2007.
46. **You G, Lee WS, Barros EJG, Kanai Y, Huo TL, Khawaja S, Wells RG, Nigam SK, Hediger MA.** Molecular characteristics of Na^+-coupled glucose transporters in adult and embryonic rat kidney. *J Biol Chem* 270: 29365–29371, 1995.

Supplementary Figure 1

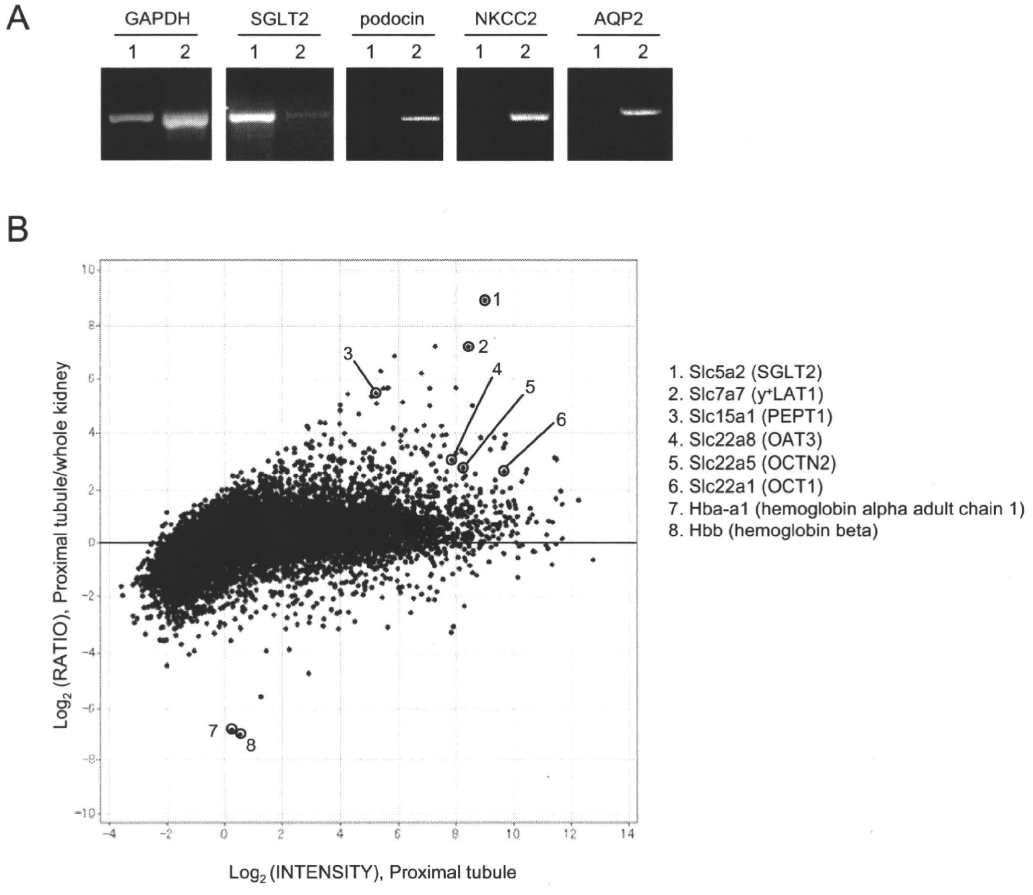

Supplementary Figure 1. Examination of the purity of the isolated proximal tubules. The expression of SGLT2, podocin, NKCC2 and AQP2 was examined by RT-PCR using the cDNA from isolated proximal tubules (1) or whole kidney (2) (**A**). The expression of SGLT2, Podocin, NKCC2 and AQP2 was used as a marker for proximal tubules, glomeruli, thick ascending limbs and collecting ducts, respectively. Microarray analysis was performed using the isolated proximal tubules and whole kidney spedimens from normal rats (**B**). The ratio of the intensity of proximal tubules to whole kidney were calculated. The genes that were reported to be expressed at the proximal tubules showed high ratio (1-6), while the genes that were not contained in the proximal tubules showed low value (7 and 8). SGLT, Na^+/glucose cotransporter; NKCC, Na^+-K^+-Cl^- cotransportery; AQP, aquaporin; y^+LAT, y(+)L-type amino acid transporter; PEPT, H^+/peptide transporter; OAT, organic anion transporter; OCTN, organic cation/carnitine transporter; OCT, organic cation transporter.

Supplementary Figure 2

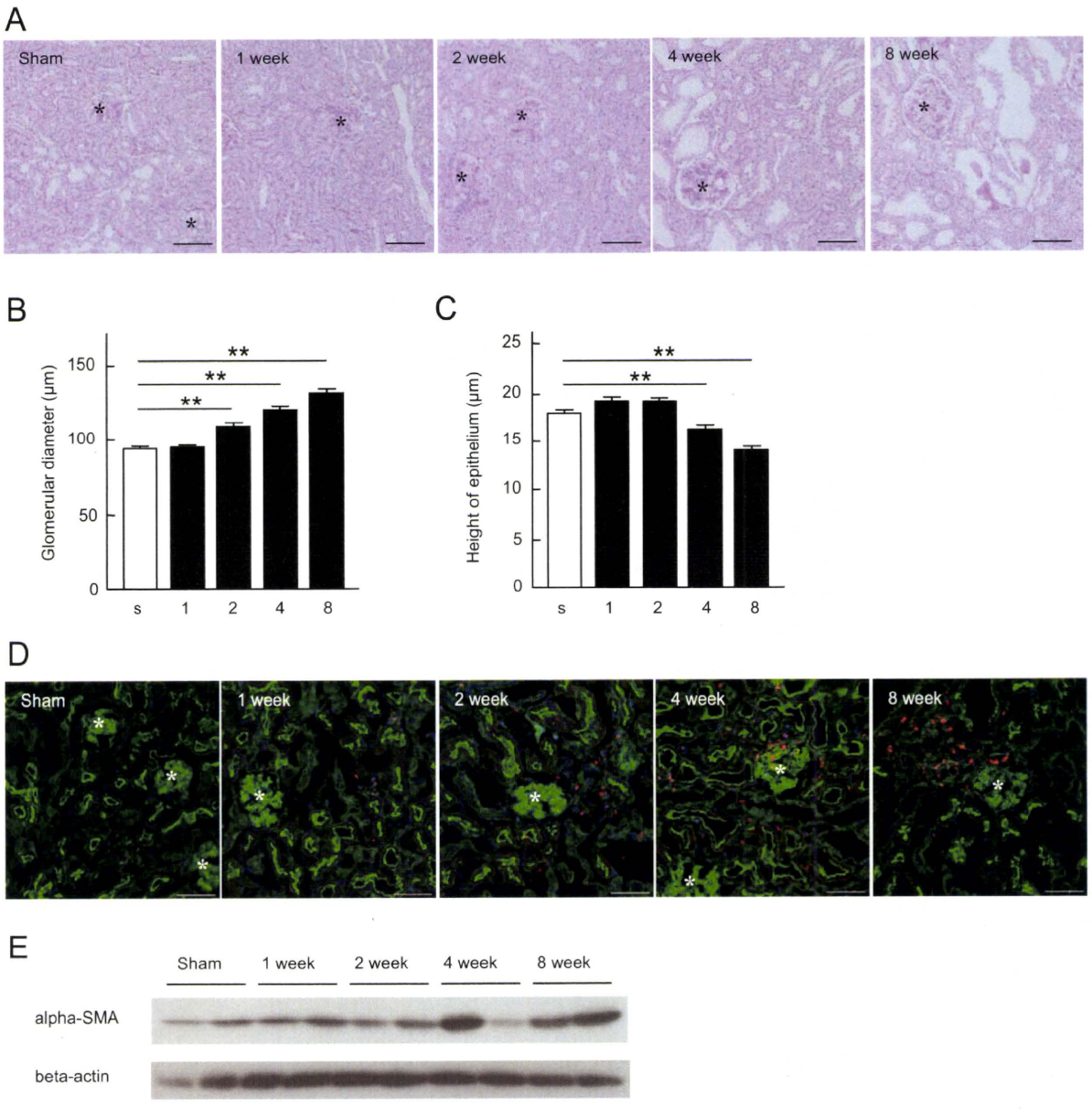

Supplementary Figure 2. Evaluation of progressive renal failure in Nx rats. The kidney was fixed in ethyl Carnoy's solution and stained with periodic acid-Schiff's reagent (**A**). *, glomeruli. Scale bar; 100 μm. Measurement of glomerular diameter in sham-operated and Nx rats at 1, 2, 4 and 8 weeks after surgery (**B**). The glomerular diameter was not changed at 1 week after Nx compared to sham-operated rats, and it was significantly increased in Nx rats at 2, 4 and 8 weeks after surgery with time after surgery. Multiple comparisons were performed with Dunnett's two-tailed test after a one-way ANOVA. ** $P < 0.01$, significantly different from sham-operated rats. The height of epithelial cells were measured (**C**). It was tended to increase in 1 and 2 weeks after Nx, but it was significantly decreased in 4 and 8 weeks after Nx. Immunofluorescent analysis of ED1 (**D**). No signal was observed in sham-operated rats. The signals were gradually increased in tubulointerstitial space in Nx rats at 1 and 2 weeks after surgery. Strong signals for ED1 in the glomeruli and tubulointerstitial space were observed in Nx rats at 4 and 8 weeks after surgery. Immunoblotting of alpha-SMA in sham-operated and Nx rats (**E**). The levels of alpha-SMA were comparable between sham-operated and Nx rats in 1 and 2 weeks after Nx, while those were markedly increased in 4 and 8 weeks after Nx.

Supplementary Figure 3

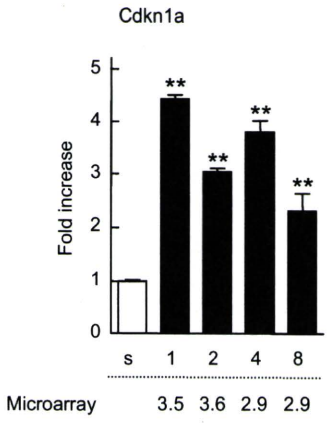

Supplementary Figure 3. Expression profile of cyclin-dependent kinase inhibitor 1a (Cdkn1a/p21$^{WAF1/Cip1}$). An equal amount of cDNA was pooled from the remnant kidney of each rat, and the expressional changes of mRNA were measured by real-time PCR and analyzed by the delta-delta Ct method. The numbers below each column show the fold change in the microarray analysis. s, sham-operated rats; 1, 2, 4, and 8, Nx rats at 1, 2, 4, and 8 weeks after surgery. Multiple comparisons were performed with Dunnett's two-tailed test after a one-way ANOVA. ** $P < 0.01$, significantly different from sham-operated rats.

Supplementary Figure 4

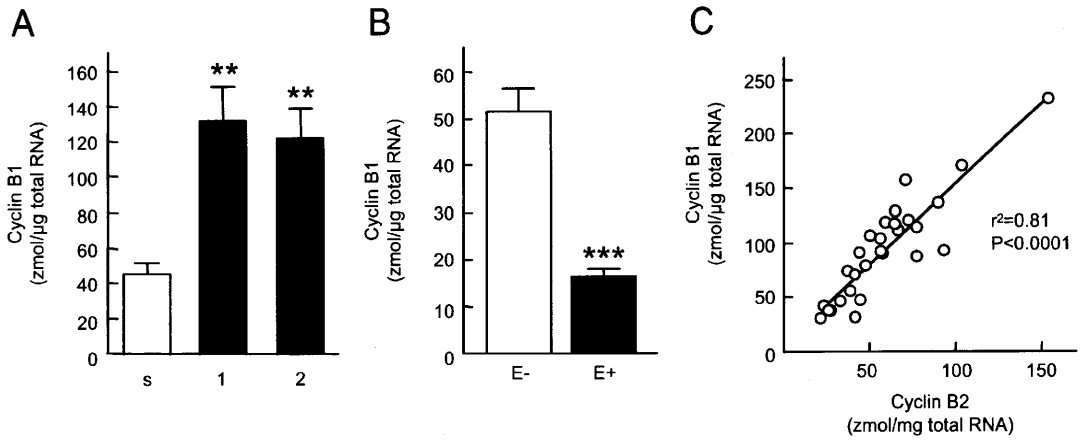

Supplementary Figure 4. Detection of the mRNA level of Cyclin B1 in the kidney. The effect of subtotal nephrectomy on the mRNA level of Cyclin B1 (**A**). s, sham-operated rats; 1 and 2, Nx rats at 1 and 2 weeks after surgery. Multiple comparisons were performed with Dunnett's two-tailed test after a one-way ANOVA. ** $P < 0.01$, significantly different from sham-operated rats. The effect of everolimus on the mRNA level of Cyclin B1 in Nx rats (**B**). E–, Nx rats treated with the vehicle; E+, Nx rats treated with everolimus. *** $P < 0.001$, significantly different from vehicle treated (E–) rats. Correlation between the mRNA levels of Cyclin B2 and Cyclin B1 in sham-operated and Nx rats (**C**). Linear regression analysis was performed and the correlation coefficient (r) was calculated.

Supplementary Figure 5

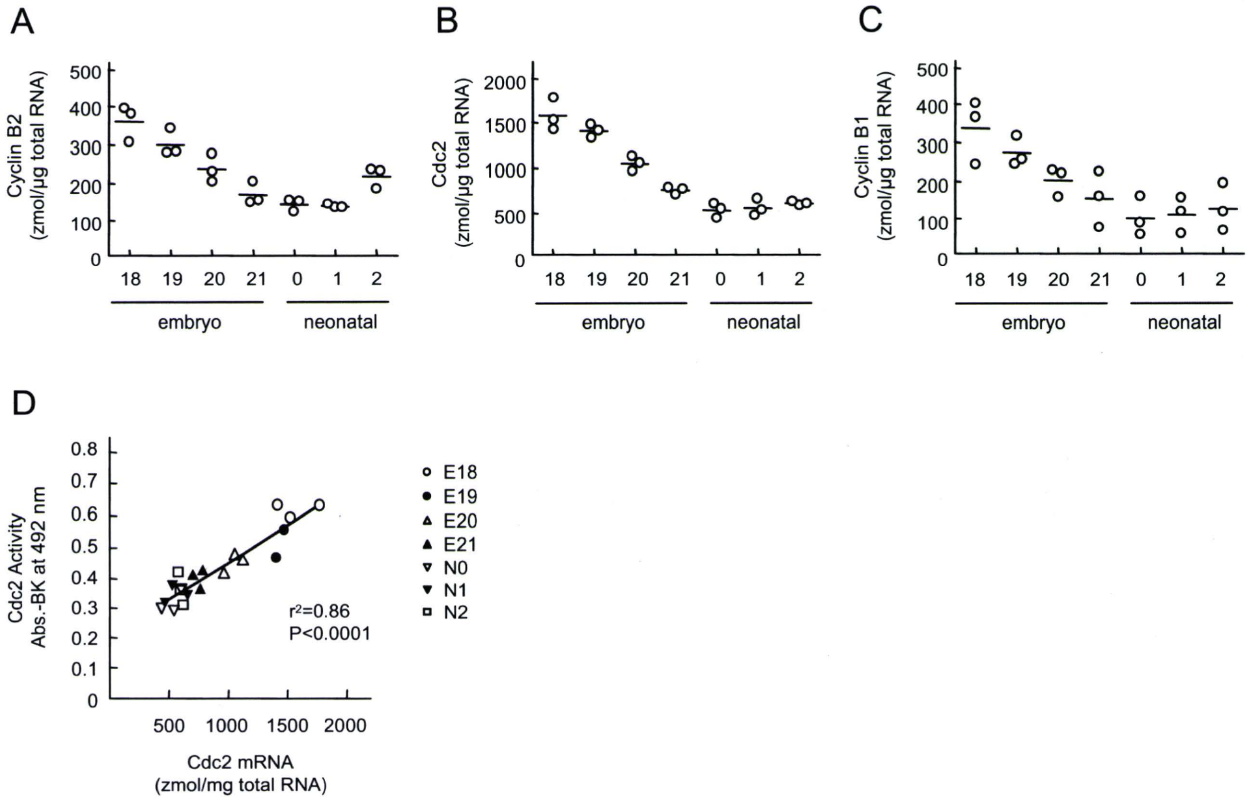

Supplementary Figure 5. Expression of Cyclin B2, Cdc2 and Cyclin B1 and the activity of Cdc2 in the embryonic and neonatal kidney. Wistar/ST rats at various stages of gestation were purchased and the kidneys were collected. We used three separate batches of maternal rats. The mRNA levels of Cyclin B2 (**A**), Cdc2 (**B**) and Cyclin B1 (**C**) were measured by real-time PCR. The levels of Cyclin B2, Cdc2 and Cyclin B1 were high in the embryonic and neonatal kidney and decreased with growth. The correlation between the activity and mRNA expression of Cdc2 in embryonic and neonatal kidney (**D**). The linear regression analysis was performed and the correlation coefficient (r) was calculated. E, embryonic day; N, neonatal day.

Supplementary methods

Examination of the purity of the isolated proximal tubules by RT-PCR and microarray analysis

Total RNA was extracted from the isolated proximal tubules or whole kidney specimens of normal rats using RNeasy Mini Kit (QIAGEN). The total RNA was reverse transcribed using the High Capacity cDNA Reverse Transcription Kit (Applied Biosystems) and subjected to digestion with RNase H (Invitrogen Co., Carlsbad, CA). After dilution of reaction mixture, the expression of SGLT2, podocin, NKCC2, AQP2 and GAPDH was examined by RT-PCR using the aliquots of cDNA. Following the denaturing of the single-strand DNA at 95°C for 3 min, RCR was performed: 94°C for 1 min, 55°C for 1 min (podocin, NKCC2 and AQP2) or 65°C for 1 min (SGLT2) or 60°C for 1 min (GAPDH), 72°C for 1 min for 30 cycles. The primer sets used for RT-PCR were referred to previous reports (SGLT2 and GAPDH (3); podocin (1); NKCC2 and AQP2 (2)). The expression of GAPDH was examined as internal control. The expressional profiles in isolated proximal tubules and whole kidney were compared by microarray analysis. The labeling reaction, array hybridization, chemiluminescence detection, and image acquisition were performed as described in **Materials and Methods** section.

Immunoblot analysis

The kidney was homogenized in a lysis buffer containing 1% NP-40, 50 mM Tris-HCl (pH 7.5), 150 mM NaCl, 10 mM NaF, 1 mM sodium pyrophosphate, 1 mM Na_3VO_4, and protease inhibitor cocktail (Nacalai Tesque, Kyoto, Japan). The whole-kidney lysate was centrifuged at 10,000 × g at 4°C for 15 min. The supernatant

was collected, and the protein concentration was determined. The lysate (50 μg) was separated by SDS-polyacrylamide gel electrophoresis and transferred onto polyvinylidene difluoride membranes. After blocking the membrane, the blots were incubated with antisera against alpha-SMA or beta-actin (Sigma-Aldrich). The bound antibody was detected on X-ray film by enhanced chemiluminescence (ECL) with horseradish peroxidase-conjugated secondary antibodies and cyclic diacylhydrazides (GE Healthcare Bio-Sciences Corp., Piscataway, NJ, USA). The levels of beta-actin were examined as internal control.

Real-time RCR in embryonic and neonatal kidney

In the case of embryonic and neonatal kidney, Wistar/ST rats at various stages of gestation were purchased from Shimizu Laboratory Supplies Co., Ltd. (Kyoto, Japan); the kidneys were then collected from 9 to 12 embryos of the same maternal rat. We used three separate batches of maternal rats.

References

1. **Kawachi H, Koike H, Kurihara H, Sakai T, Shimizu F**. Cloning of rat homologue of podocin: Expression in proteinuric states and in developing glomeruli. *J Am Soc Nephrol* 13: 46-56, 2003.
2. **Nishimura M, Kakigi A, Takeda T, Takeda S, Doi K**. Expression of aquaporins, vasopressin type 2 receptor, and Na^+-K^+-Cl^- cotransporters in the rat endolymphatic sac. *Acta Oto-Laryngologica* 129: 812-818, 2009.
3. **Takahashi K, Masuda S, Nakamura N, Saito H, Futami T, Doi T, Inui K**. Upregulations of H^+-peptide cotoransporter PEPT2 in rat remant kidney. *Am J*

Physiol Renal Physiol 281: F1109-1116, 2001.

Biochemical Pharmacology 79 (2010) 67–76

Contents lists available at ScienceDirect

Biochemical Pharmacology

journal homepage: www.elsevier.com/locate/biochempharm

mTOR inhibitor everolimus ameliorates progressive tubular dysfunction in chronic renal failure rats

Shunsaku Nakagawa, Satohiro Masuda, Kumiko Nishihara, Ken-ichi Inui *

Department of Pharmacy, Kyoto University Hospital, Faculty of Medicine, Kyoto University, Sakyo-ku, Kyoto 606-8507, Japan

ARTICLE INFO

Article history:
Received 16 June 2009
Accepted 28 July 2009

Keywords:
Mammalian target of rapamycin
Proximal tubule injury
Albuminuria
Drug transporter
Chronic kidney disease

ABSTRACT

Responsible factors in progressive tubular dysfunction in chronic renal failure have not been fully identified. In the present study, we hypothesized that the mammalian target of rapamycin, mTOR, was a key molecule in the degenerative and progressive tubular damage in chronic renal failure. Everolimus, an mTOR inhibitor, was administered for 14 days in 5/6 nephrectomized (Nx) rats at 2 and 8 weeks after renal ablation. Marked activation of the mTOR pathway was found at glomeruli and proximal tubules in remnant kidneys of Nx rats. The reduced expression levels of the phosphorylated S6 indicated the satisfactory pharmacological effects of treatment with everolimus for 14 days. Everolimus suppressed the accumulation of smooth muscle alpha actin, infiltration of macrophages and expression of kidney injury molecule-1 in the proximal tubules. In addition, everolimus-treatment restored the tubular reabsorption of albumin, and had a restorative effect on the expression levels of membrane transporters in the polarized proximal tubular epithelium, when its administration was started at 8 weeks after Nx. These results indicate that the constitutively activated mTOR pathway in proximal tubules has an important role in the progressive tubular dysfunction, and that mTOR inhibitors have renoprotective effects to improve the proximal tubular functions in end-stage renal disease.

1. Introduction

In chronic renal failure (CRF), the irreversible and progressive loss of nephrons ultimately results in glomerular sclerosis, tubular atrophy and further reductions in nephron numbers [1,2]. These physiological changes produce a complex series of adverse effects that eventuate in progressive renal injury and a severe decline in function. We have demonstrated expressional and functional alterations of drug transporters in the proximal tubules of 5/6 nephrectomized (Nx) rats, a model of CRF [3–6]. Furthermore, levels of tubular transporters that play important roles in the handling of nutrients and electrolytes were also decreased in Nx rats [7,8]. Therefore, a decline in tubular functions causes the accumulation of uremic toxin, metabolites and xenobiotics and increases renal dysfunction and systemic toxicity [9,10]. Consequently, it is important to understand the molecular mechanisms behind in CRF and improve therapeutic approaches for the progressive tubular dysfunction.

Mammalian target of rapamycin, mTOR, is a serine/threonine kinase that regulates a variety of cellular processes including growth, proliferation and metabolism [11–13]. mTOR inhibitors such as rapamycin (sirolimus) and everolimus are generally used as immunosuppressants to prevent immunological reactions after organ transplantation. Everolimus is an immunosuppressive macrolide derived from rapamycin. Although they exhibit slightly different pharmacokinetic properties, both everolimus and rapamycin exert their effects by the same mechanism [12]. Each drug binds to the intracellular cofactor FK506-binding protein (FKBP12) to form a complex, which then binds to mTOR interfering signal transduction to its downstream effectors.

Recently, it was reported that rapamycin reduced interstitial fibrosis and glomerular sclerosis after kidney transplantation in patients with chronic allograft nephropathy [14,15]. In addition, a causal link between the activation of the mTOR pathway and the progression of polycystic kidney disease or diabetic nephropathy was reported [16–18]. However, it is still unclear whether the mTOR pathway associates with tubular functions such as the reabsorption of nutrients and secretion of xenobiotics and metabolites.

Previous studies suggest the relationship between the mTOR pathway and the progression of CRF. Diekmann et al. [19] reported that rapamycin abolished the progression of proteinuria and structural damage when administered from the 6th week after nephrectomy in CRF rats, while Vogelbacher et al. [20] reported that everolimus induced renal deterioration and proteinuria when given from the 3rd day after nephrectomy. These findings encouraged us to examine the pharmacological effects of everolimus in Nx rats,

* Corresponding author. Tel.: +81 75 751 3577; fax: +81 75 751 4207.
E-mail address: inui@kuhp.kyoto-u.ac.jp (K.-i. Inui).

0006-2952/$ – see front matter © 2009 Elsevier Inc. All rights reserved.
doi:10.1016/j.bcp.2009.07.015

focusing on tubular functions, by subcutaneously administration of everolimus at 2 and 8 weeks after renal ablation. Our findings revealed the constitutive activation of the mTOR pathway at proximal tubules in the remnant kidneys, and the therapeutic effects of everolimus for the progression of tubular dysfunction in CRF.

2. Materials and methods

2.1. Animals

The experimental design is shown in Fig. 1. For ablation of the renal mass, male Wistar/ST rats (180–200 g) were anesthetized with sodium pentobarbital (50 mg/kg) and the kidneys were exposed under aseptic conditions via a ventral abdominal incision. The right kidney was removed, the posterior and anterior apical segmental branches of the left renal artery were individually ligated, and the abdominal incision was closed with 4-0 silk sutures [3,4]. After surgery, animals were allowed to recover from anesthesia and surgery in cages with free access to water and standard rat chow. To investigate the effects of the mTOR inhibitor everolimus on the progression of CRF, rats were administered everolimus (LC Laboratories, Woburn, MA; 2 mg/kg body weight, E(+)) or vehicle (E(−)) subcutaneously for 14 days. The administration of everolimus was initiated at 2 and 8 weeks after surgery. After the 14-day administration, the subsequent experiments were carried out. The concentration of everolimus in whole blood samples was measured using LC/MS/MS [21]. The experiments with animals were performed in accordance with the *Guidelines for Animal Experiments of Kyoto University*. All protocols were previously approved by the Animal Research Committee, Graduate School of Medicine, Kyoto University.

2.2. Renal function and histology

Rats were maintained in metabolic cages for 24 h to collect 24-h urine samples. The animals were fed normal pellet food ad libitum, and given water freely in metabolic cages. Then, rats were anesthetized with an intraperitoneal administration of 50 mg/kg sodium pentobarbital to collect plasma and kidneys. Urinary albumin was assessed using an enzyme-linked immunosorbent assay (ELISA) kit (Nephrat II) (Exocell, Inc., Philadelphia, PA). The levels of creatinine in plasma and urine were determined with the Jaffé reaction. The BUN concentration was determined by the urease/indophenol method. For measurements, we used assay kits from Wako Pure Chemical Industries (Osaka, Japan). Kidneys were fixed in ethyl Carnoy's solution and stained with periodic acid-Schiff (PAS) reagent by Sapporo General Pathology Laboratory Co., Ltd. (Hokkaido, Japan). The glomerular diameter and inside diameter of tubules were determined as the mean value from 20 glomeruli and 40 proximal tubules, respectively.

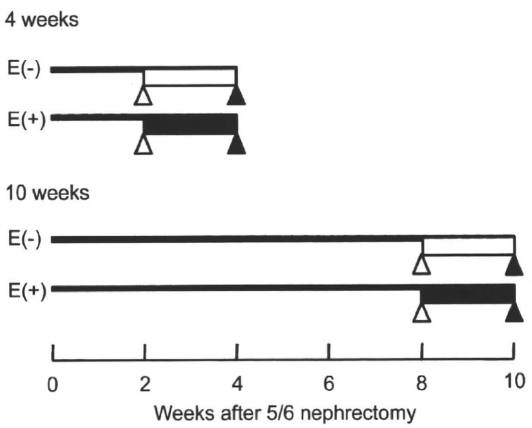

Fig. 1. Experimental design. Rats were administered everolimus (2 mg/kg body weight, E(+)) or vehicle E(−)) subcutaneously for 14 days. The trough concentration of everolimus at the 15th day was 18.4 ± 1.2 ng/mL. The administration of everolimus was initiated at 2 and 8 weeks after 5/6 nephrectomy. Open triangle, initiation of administration; closed triangle, sample collection; open bar, administration of vehicle; closed bar, administration of everolimus.

2.3. Western blot analysis

The rat whole kidney was homogenized in lysis buffer (50 mM Tris–HCl, pH 7.5, 150 mM NaCl, 10 mM NaF, 1 mM $Na_4P_2O_7$, 100 mM Na_3VO_4, 1% NP-40 and 1% protease inhibitor cocktail (Nacalai Tesque, Kyoto, Japan)). The tissue lysate was clarified by centrifugation, and protein concentrations were determined with the Bradford protein assay (Bio-Rad Laboratories, Hercules, CA). The crude membrane fractions of the rat kidney were prepared as described [22]. The kidney lysate was used for the analyze the protein levels of phosphorylated Akt (p-Akt), mTOR (p-mTOR), S6 kinase (p-S6 kinase), ribosomal protein S6 (p-S6), kidney injury molecule-1 (Kim-1), smooth muscle alpha actin (alpha-SMA), beta-actin and GAPDH. The membrane fraction was used for Na^+/D-glucose cotransporter (SGLT) 1, Na^+/H^+ exchanger (NHE) 3, H^+/peptide cotransporter (PEPT) 1, PEPT2, organic cation transporter (OCT) 1, OCT2 organic anion transporter (OAT) 1, OAT3, H^+/organic cation antiporter (MATE, multidrug and toxin extrusion) 1, P-glycoprotein (P-gp) and the Na^+/K^+-ATPase alpha1 subunit. Equal amount of the lysate or membrane fraction was separated by sodium dodecyl sulfate-polyacrylamide gel electrophoresis (SDS-PAGE) and transferred to polyvinylidene difluoride (PVDF) membranes (Millipore, Billerica, MA). The blots were blocked, washed, and incubated with the primary antibodies (for total Akt, p-Akt, total mTOR, p-mTOR, p-S6K, total S6, p-S6 (Cell Signaling Technology, Danvers, MA), GAPDH (Santa Cruz Biotechnology, Avenue, CA), alpha-SMA, beta-actin (Sigma), Kim-1 (generated in our laboratory referring to the report by Ichimura et al. [23], Fig. 2),

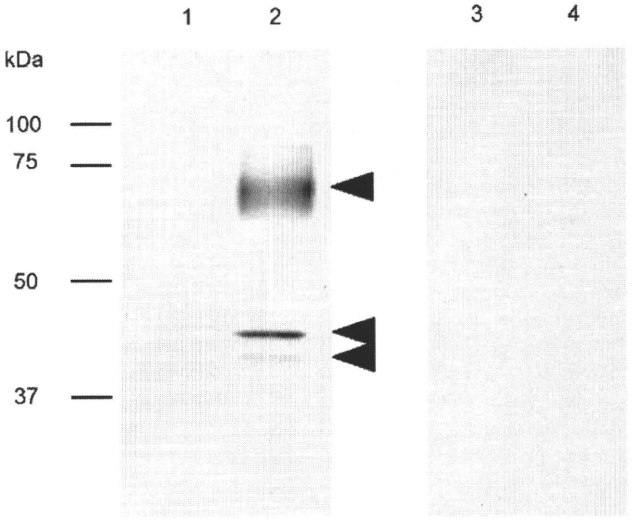

Fig. 2. Polyclonal antibody against Kim-1. Polyclonal antibody was raised against the synthetic peptide corresponding to the R9 region of rat Kim-1 (HPRAEDNIYIIEDRSRG) [23]. Tissue lysates (50 μg) from normal kidney (lanes 1 and 3) or Nx rat kidneys at 10 weeks after surgery (lanes 2 and 4) were separated by SDS-PAGE and blotted onto PVDF membranes. Antibody specific for Kim-1 (lanes 1 and 2) or antibody preabsorbed with the synthetic antigen peptide (10 μg/mL) (lanes 3 and 4) were used as primary antibody. Kim-1 protein was up-regulated in the Nx rat kidneys. The preabsorption of antibody with corresponding antigen peptide abolished these positive bands, showing the presence of Kim-1 protein in the rat kidney. Arrows indicate the position of the Kim-1 specific bands.

SGLT1, NHE3, Na^+/K^+-ATPase alpha1 subunit (Millipore), PEPT1 [24], PEPT2 [25], OCT1 [26], OCT2 [27], OAT1, OAT3 [4], MATE1 [6] and P-gp (monoclonal antibody C219 [28])) overnight at 4 °C. The bound antibody was detected on X-ray film by enhanced chemiluminescence (ECL) with horseradish peroxidase-conjugated secondary antibodies and cyclic diacylhydrazides (GE Healthcare Bio-Sciences Corp., Piscataway, NJ). Beta-actin, GAPDH and the Na^+/K^+-ATPase alpha1 subunit were examined as controls. The relative densities of the bands in each lane were determined using NIH Image J 1.39 (National Institute of Health, Bethesda, MD, USA).

2.4. Immunofluorescence analysis

Rats at 15th days after the daily administration of everolimus or vehicle from 2 or 8 weeks after surgery were used. After perfusion with 4% paraformaldehyde in PBS (Wako), and the kidneys were embedded in Tissue-Tek® O.C.T. compound (Sakura Finetechnical, Tokyo, Japan) and frozen rapidly in liquid nitrogen. Sections (6 μm thick) were cut and covered with 5% BSA in PBS containing 0.3% Triton X-100. The covered sections were incubated for overnight at 4 °C with the primary antibodies (1:200 dilution) specific for p-mTOR, p-S6, alpha-SMA, ED1 and rat Kim-1 (R&D Systems, Minneapolis, MN), washing three times, and incubated with secondary antibodies (Cy3-labeled donkey anti-rabbit IgG (ALTAG Laboratory, San Francisco, CA) for p-mTOR and p-S6, Alexa 546-labeled donkey anti-goat IgG (Invitrogen Japan K.K., Tokyo, Japan) for rat Kim-1, Alexa 546-labeled goat anti-mouse IgG (Invitrogen) for ED1 and alpha-SMA), Alexa 488-Phalloidin (Invitrogen), and DAPI (Wako, Osaka, Japan) at 37 °C for 60 min. These sections were examined under a fluorescence microscope BZ-9000 (KEYENCE, Osaka, Japan). Signals for secondary antibodies, Alexa 488-Phalloidin and DAPI were captured, and the images of each color signals in the same section were merged.

2.5. Infusion experiment

Renal distribution of fluorescein isothiocyanate-conjugated human albumin (FITC-albumin; Sigma, Deisenhofen, Germany) was measured in rats at 15th days after the daily administration of everolimus or vehicle from 8 weeks after surgery. Rats were anesthetized with an intraperitoneal administration of 50 mg/kg sodium pentobarbital, and catheterized at right femoral vein for the administration of FITC-albumin. Urine was collected from the urinary bladder catheterized with the tubing (Intramedic PE-50, Becton Dickinson and Co., Parsippany, NJ). Thereafter, FITC-albumin (5 mg/kg) was administered as a bolus via the femoral vein. Urine samples were collected during a 20-min period, and then, the kidneys were harvested. The FITC-albumin concentrations in urine were determined with an ELISA kit (AssayMax Human Albumin ELISA Kit) (ASSAYPRO, Triad South Drive St. Charles, MO). Fixed kidneys were frozen rapidly in liquid nitrogen. Sections (6 μm thick) were cut and incubated with Alexa 594-Phalloidin (Invitrogen) at 37 °C for 30 min. Signals for FITC-albumin or Alexa 594-Phalloidin were captured with a BZ-9000. Area of signals for FITC-albumin was calculated in three independent fields of renal cortex from six independent rats. The images of FITC-albumin and Alexa 594-Phalloidin in the same section were merged.

2.6. Statistical analysis

Data are expressed as means ± SEM. Data were statistically analyzed using the unpaired Student's *t*-test or multiple comparisons with Bonferroni's two-tailed test after a one-way ANOVA. Probability values of less than 0.05 were considered statistically significant. Statistical analysis was performed using Prism Version 4.0 software (GraphPad, San Diego, CA).

3. Results

3.1. Protein expression of phosphorylated Akt, mTOR, S6 kinase and S6

The phosphatidylinositol 3-kinases (PI3K)/Akt pathway is an upstream regulator of mTOR, and the activation of mTOR leads to the phosphorylation of downstream targets, such as S6 kinase and S6 [11,12]. After the 14 days' subcutaneous administration of everolimus (Fig. 1), the protein levels of p-Akt, p-mTOR, p-S6 kinase, p-S6 in the Nx rat kidneys were examined (Fig. 3). Although slight variations in the levels of total Akt, mTOR and S6 were observed, the levels of p-Akt, p-S6 kinase and p-S6 as well as p-mTOR were markedly increased in Nx rat kidneys compared to the control rat kidney (Fig. 3, Control vs. 4 weeks E(−) or 10 weeks E(−)). The treatment with everolimus markedly decreased the levels of p-S6 kinase and p-S6 (Fig. 3, 4 weeks E(−) vs. E(+), 10 weeks E(−) vs. E(+)). In addition, the levels of p-Akt and p-mTOR tended to decrease on treatment with everolimus, when the administration was started at 8 weeks after surgery (Fig. 3, 10 weeks E(−) vs. E(+)).

An immunofluorescence analysis revealed extensive staining of p-mTOR and p-S6 in the renal cortex (Fig. 4A–F). In the control rat kidneys, the signals for p-mTOR were predominantly observed in distal tubules (Fig. 4A, arrowhead), while the signals for p-S6 were observed in proximal tubules (Fig. 4B, arrow) as well as distal tubules (Fig. 4B, arrowhead). In the remnant kidneys, the staining

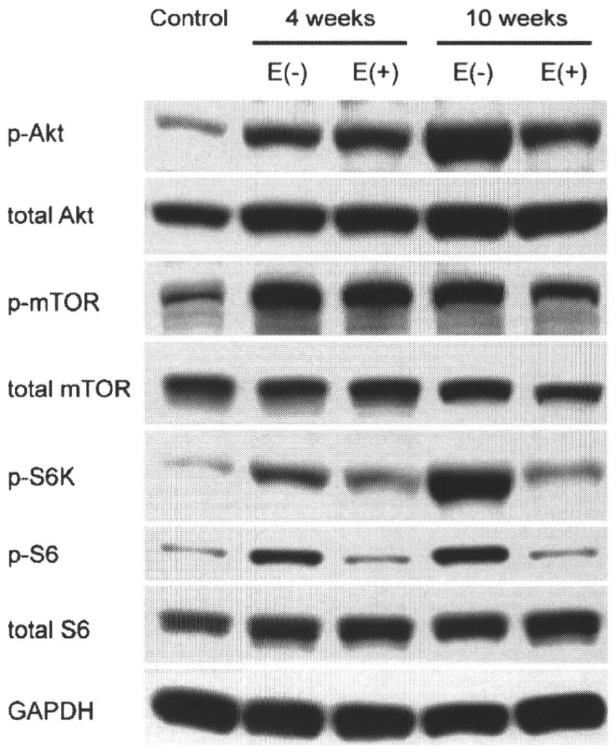

Fig. 3. Activation of the mTOR pathway in Nx rat kidneys. Four weeks and 10 weeks represent groups in which a 14-day subcutaneous administration of everolimus (2 mg/kg/day) or vehicle was initiated at 2 and 8 weeks after surgery, respectively. Tissue lysate (50 μg) from total kidney was separated by SDS-PAGE and blotted onto PVDF membranes. Antisera specific for total Akt, p-Akt, total mTOR, p-mTOR, p-S6 kinase total S6, p-S6 and GAPDH (1:1000–4000 dilution) were used as primary antibody. Control, lysate obtained from normal kidney; E(−), Nx rats administered vehicle; E(+), Nx rats administered everolimus.

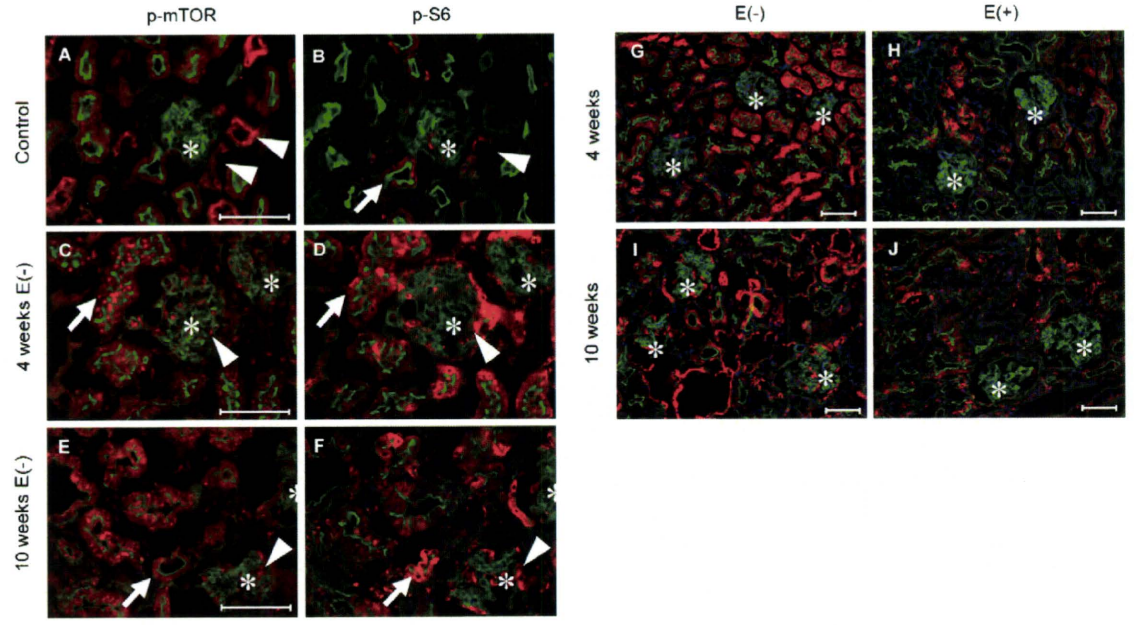

Fig. 4. Immunofluorescence analysis for p-mTOR and p-S6. (A–F) Serial sections of Nx rat kidneys are shown. Red signals for p-mTOR (A, C and E) or p-S6 (B, D and F) were merged with green signals for F-actin. (G–J) Effects of everolimus on the expression levels of p-S6 in Nx rats. Red signals for p-S6 were merged with green signals for F-actin and blue signals for DAPI. Symbols (*) represent the localization of glomeruli. Each scale bar represent a length of 100 μm. E(−), Nx rats administered vehicle; E(+), Nx rats administered everolimus.

of p-mTOR and p-S6 was intensified and aggregated in glomeruli (Fig. 4C–F, arrowheads) and the proximal tubular epithelial cells (Fig. 4C–F arrows). However, treatment with everolimus markedly decreased the intensity and area of signals for p-S6 (Fig. 4G–J).

3.2. Effects of everolimus on renal functions in Nx rats

As summarized in Table 1, significant changes in the kidney/body weight ratio, the urinary excretion of albumin (Ualb), and creatinine clearance (Ccr) and an increase in the level of blood urea nitrogen (BUN) were observed with time after renal ablation. When everolimus was administered daily for 14 days beginning at 2 weeks after surgery, significant decreases in Ccr and body weight were observed (Table 1, 4 weeks E(−) vs. E(+)). Although statistically not significant, the level of BUN tended to be increased by the administration of everolimus (Table 1, 4 weeks E(−) vs. E(+)). The kidney/body weight ratio and urinary excretion of albumin were markedly decreased when the administration of everolimus was initiated at 8 weeks after surgery, but the Ccr, level of BUN, body weight and urine volume were not affected by the administration of everolimus (Table 1, 10 weeks E(−) vs. E(+)).

3.3. Renal histology

Fig. 5A–D shows paraffin-embedded sections stained with PAS reagent. The glomerular diameter and inside diameter of tubules increased with time after the surgery (Fig. 5E and F, 4 weeks E(−) vs. 10 weeks E(−)). Glomerular hypertrophy and loss of the brush-border also progressed with time after renal ablation. However, these parameters were significantly decreased by the treatment with everolimus (Fig. 5E and F, 4weeks E(−) vs. E(+), 10 weeks E(−) vs. E(+)).

Strong signals for alpha-SMA and ED1 in the glomeruli (Fig. 6A, C, E and G; arrows) and tubulointerstitial space (Fig. 6A, C, E and G; arrowheads) were observed following Nx. However, the intensity of signals for alpha-SMA and the number of signals for ED1 decreased after the administration of everolimus (Fig. 6B, D, F and H). Furthermore, the expression levels of Kim-1 decreased after the administration of everolimus from 8 weeks after surgery (Fig. 6L), while proximal tubule-specific expression of Kim-1 increased with time after the surgery (Fig. 6I and K). Western blot analysis clearly showed that the expressional changes of alpha-SMA and Kim-1 were comparable with that observed in the immunofluorescence examination (Fig. 6M).

Table 1
Biochemical parameters in Nx rats.

	4 weeks		10 weeks	
	E(−)	E(+)	E(−)	E(+)
Body weight (g)	296 ± 15	242 ± 11*	361 ± 23	333 ± 18
Urine volume (mL/day)	33.1 ± 1.6	37.9 ± 3.5	31.8 ± 2.0	34.5 ± 4.5
Kidney weight/Body weight (%)	0.35 ± 0.03	0.27 ± 0.02	0.47 ± 0.04§	0.32 ± 0.01††
Ccr (mL/min/kg)	3.34 ± 0.51	1.61 ± 0.33*	1.32 ± 0.38§§	0.90 ± 0.29
BUN (mg/dL)	53.9 ± 8.7	111.4 ± 15.0	119.1 ± 31.3	120.7 ± 17.2
Ualb (mg/day)	46.5 ± 15.9	51.1 ± 16.3	128.7 ± 28.8§	45.6 ± 6.7†

Values are the mean ± SEM for six rats. Rats of 4 weeks and 10 weeks represent groups in which a 14-day subcutaneous administration of everolimus (2 mg/kg/day) or vehicle was initiated at 2 and 8 weeks after surgery, respectively. Ccr, creatinine clearance; BUN, blood urea nitrogen; Ualb, urinary albumin excretion; E(−), 5/6 nephrectomized rats administered vehicle; E(+), 5/6 nephrectomized rats administered everolimus. *$P < 0.05$, §$P < 0.05$, §§$P < 0.01$, significantly different from E(−) rats at 4 weeks. †$P < 0.05$, ††$P < 0.01$, significantly different from E(−) rats at 10 weeks.

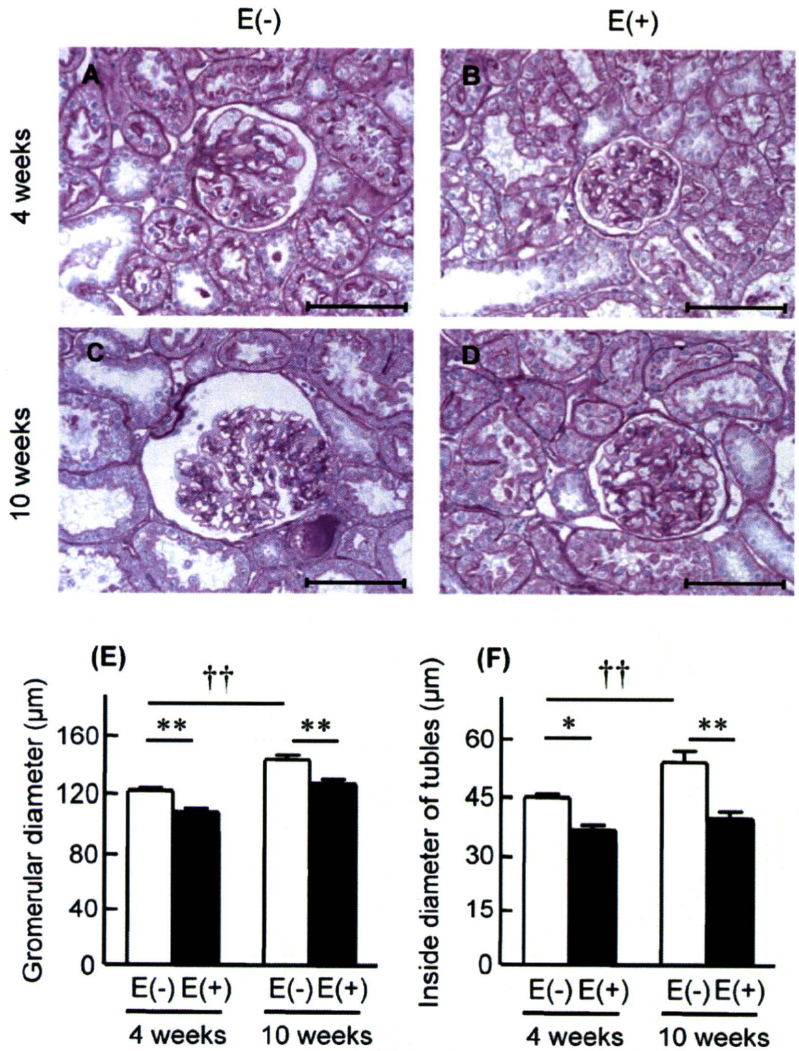

Fig. 5. Histological analysis of Nx rat kidneys. Four weeks and 10 weeks represent groups in which a 14-day subcutaneous injection was initiated at 2 and 8 weeks after surgery, respectively. (A–D) Representative photographs of PAS staining are shown. (E and F) Glomerular hypertrophy and tubular dilatation were assessed as described in the methods section. E(−), Nx rats administered vehicle; E(+), Nx rats administered everolimus. $^{\dagger\dagger}P < 0.01$, $^{*}P < 0.05$, $^{**}P < 0.01$, significantly different.

3.4. Reabsorption of FITC-albumin

Because everolimus significantly decreased the urinary excretion of albumin with minor changes in Ccr and the level of BUN (Table 1), the renal distribution of FITC-albumin was examined to visualize the restored reabsorptive function of proximal tubules (Fig. 7). The urinary FITC-albumin/creatinine ratio was significantly decreased to 31% in the Nx rats by treatment with everolimus from 8 weeks after renal ablation (Fig. 7E). Micrographs revealed green signals for FITC-albumin in the proximal tubules of the cortex where red signals for phalloidin were detected (Fig. 7A–D). In addition, the areas of green signals in the cortex were increased on the administration of everolimus (Fig. 7F), suggesting enhanced reabsorption of albumin from the filtered primary urine. In the kidneys of Nx rats administered vehicle, green signals were predominantly observed close to the brush-border membrane, with relatively weak signals detected at the side of the basolateral membrane (Fig. 7B). However, strong signals for albumin-containing vesicles were distributed throughout the proximal tubular epithelial cells in the everolimus-treated rat kidneys (Fig. 7D).

The treatment with everolimus decreased the number of proximal tubular epithelial cells positive for Kim-1 (Fig. 6), and then, we further analyzed the localization of Kim-1 in FITC-albumin administered rat kidneys (Fig. 7G and H). Immunofluorescence analysis with the antibody specific for Kim-1 showed that the injured proximal tubular epithelial cells, as indicated by red signals for Kim-1, contained little green signals for FITC-albumin (Fig. 7G and H). In contrast, tubular cells that contained strong signals for FITC-albumin were negative for Kim-1 (Fig. 7G and H).

3.5. Protein expression levels of transporters in proximal tubules

To obtain more information about the pharmacological effects of everolimus on tubular functions such as detoxicating systems and ion homeostasis, the protein levels of membrane transporters were examined (Fig. 8). Expression levels of 10 transporter proteins were depressed after surgery. Notably, the levels of NHE3, OCT1, OCT2, OAT1, OAT3, and MATE1 decreased with time after renal ablation. However, the levels of OCT1, OCT2, OAT1, OAT3 and MATE1 in the remnant kidneys after the administration of everolimus from 8 weeks after surgery were much higher than those in rats administered vehicle alone (Fig. 8, 10 weeks E(−) vs. E(+)), while everolimus tended to decrease the levels of OAT1, OAT3 and MATE1 when administered from 2 weeks after renal ablation (Fig. 8, 4 weeks E(−) vs. E(+)). In addition, the treatment with everolimus recovered the protein levels of NHE3 and PEPT2

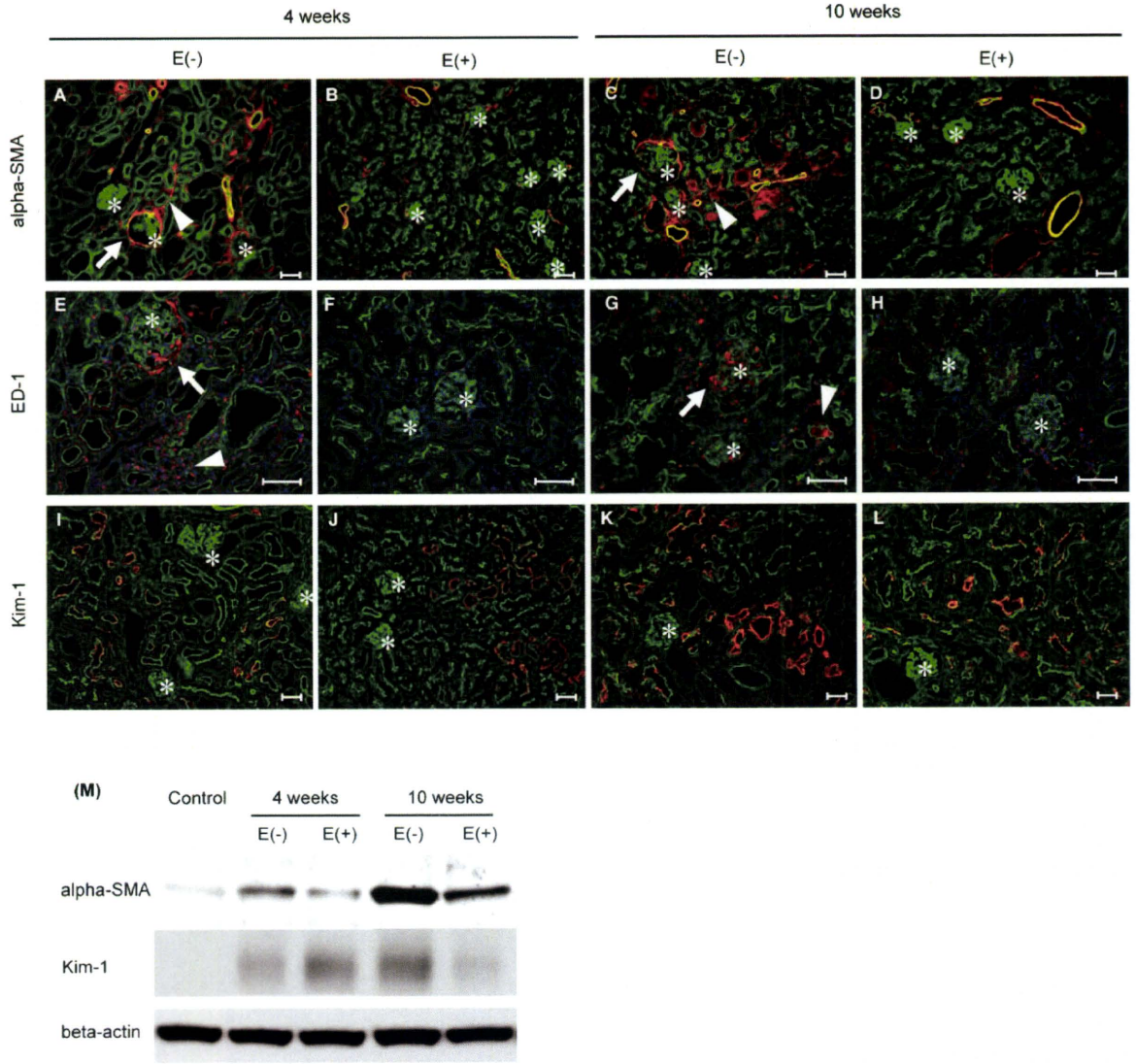

Fig. 6. Effects of the treatment with everolimus on the progression of CRF. Red signals for alpha-SMA (A-D), ED1 (E-H) and Kim-1 (I-L) in Nx rat kidneys were merged with green signals for F-actin and blue signals for DAPI. (M) Expression levels of alpha-SMA and Kim-1 were confirmed by Western blotting. Symbols (*) represent the localization of glomeruli. Scale bar: 100 μm. E(−), Nx rats administered vehicle; E(+), Nx rats administered everolimus.

independent on the timing of the initiation of treatment (Fig. 8, 4 weeks E(−) vs. E(+), 10 weeks E(−) vs. E(+)). In contrast, everolimus did not affect the levels of SGLT1, PEPT1 and P-gp. The effects of everolimus on the protein levels of membrane transporters, alpha-SMA and Kim-1 were summarized in Fig. 9.

4. Discussion

In the present study, we explored the role of mTOR pathway on the progression of CRF, and revealed the pathological significance of the mTOR pathway in the proximal tubular epithelium in CRF in vivo. Recently, the mTOR pathway has attracted attention for its roles in renal disease. It has been reported to regulate mesangial hypertrophy in diabetic nephropathy [17,18] and cyst formation in polycystic kidney disease [16,29], and to have an important role on the development of compensatory renal hypertrophy after nephron loss [30]. However, the role of the mTOR pathway in the proximal tubules was previously examined only in vitro such as using primary cultured mouse tubular cells [31] and the cultured human proximal tubule cell line, HK2 [32]. There have been no studies on its role in the progressive tubular dysfunction in CRF in vivo. In the present study, we found that the phosphrylation of Akt, mTOR, S6 kinase and S6 was enhanced in Nx rat kidneys at 4 and 10 weeks after surgery (Fig. 3), and the expression levels of p-mTOR and p-S6 were increased in glomeruli and proximal tubules (Fig. 4). In addition, the daily administration of everolimus for 14 days inhibited the activation of the mTOR pathway as indicated by the levels of p-S6 kinase and p-S6 in association with the signals for p-S6 in the proximal tubules as well as glomeruli (Figs. 3 and 4G–J). Furthermore, the treatment improved the urinary excretion of albumin and renal histology (Table 1, Figs. 5 and 7). These results indicated that the constitutively activated mTOR pathway in proximal tubules plays important roles in the progressive tubular dysfunction as well as glomerular lesions.

The aberrant albuminuria was considered to be due to the decreased reabsorption of albumin at proximal tubules as well as the increased permeability of the glomerular capillary wall [33]. Recently, it was reported that impaired tubular reabsorption of urinary albumin precedes the changes in glomerular permeability of macromolecules in early diabetic nephropathy [34]. In the

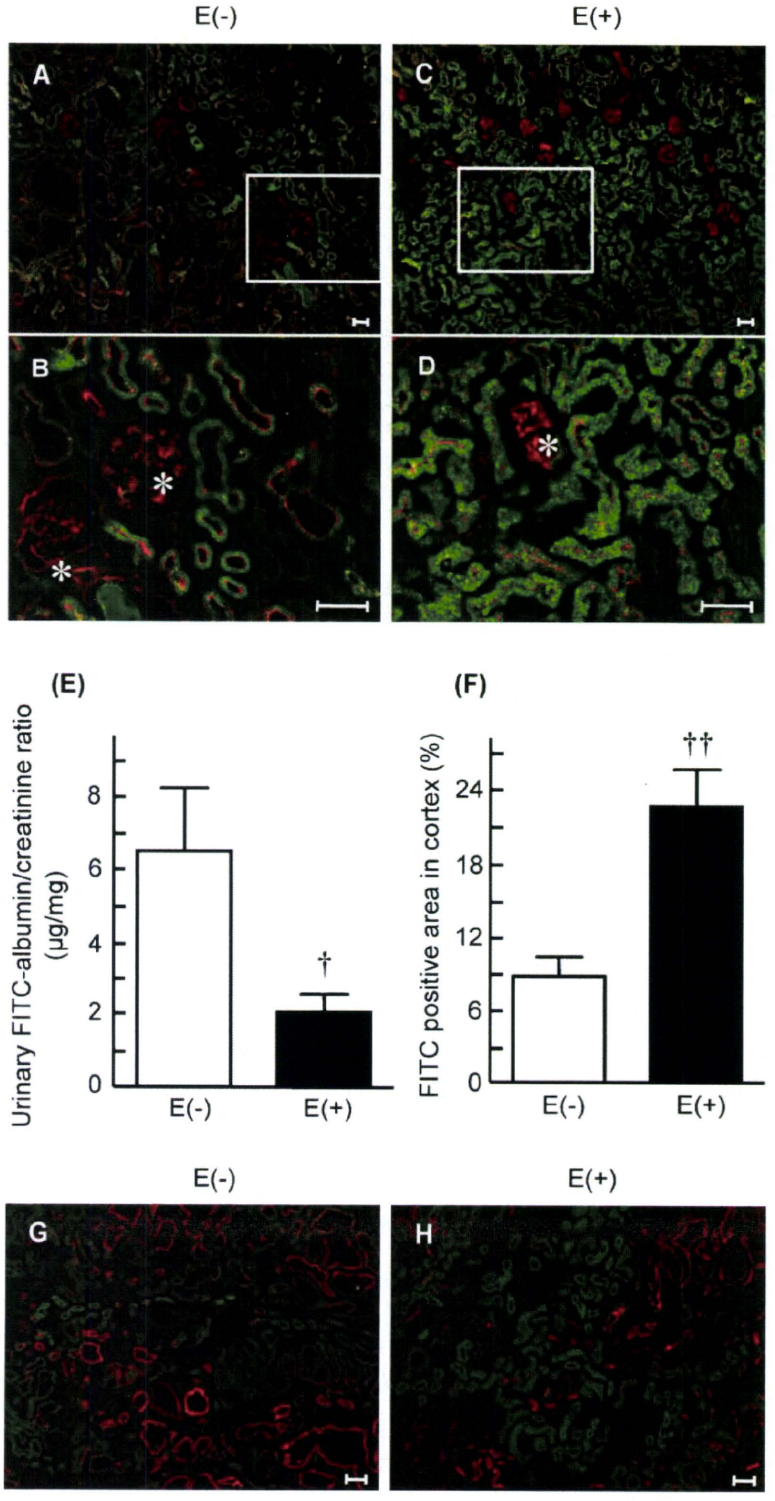

Fig. 7. Renal distribution of FITC-albumin. Nx rats 8 weeks after surgery were administered vehicle (E(−); A and B) or everolimus (2 mg/kg/day) (E(+); C and D) for 14 days. FITC-albumin (5 mg/kg) was administered as a bolus via the femoral vein. FITC (green) and F-actin (red) signals were merged in the same section. Urinary concentrations of FITC-albumin (E) and area of signals for FITC in renal cortex (F) were measured. $^{\dagger}P < 0.05$, $^{\dagger\dagger}P < 0.01$, significantly different. FITC (green) signals were merged in the same section with Kim-1 (red) signals (G and H). Scale bar: 100 μm. Symbols (*) represent the localization of glomeruli.

present study, the treatment with everolimus inhibited the progression of albuminuria (Table 1), and this phenomenon was in part due to the increase in its reabsorption at the proximal tubules (Fig. 7A–D and F) rather than the decreased permeability of the glomerular capillary wall without a marked response in glomerular function to everolimus-treatment (Table 1). On the other hand, it was reported that mTOR inhibition impaired the podocyte's integrity essential as a glomerular filtration barrier for albumin [35]. These findings and backgrounds suggest that everolimus-treatment restores the reabsorbing activity of albumin

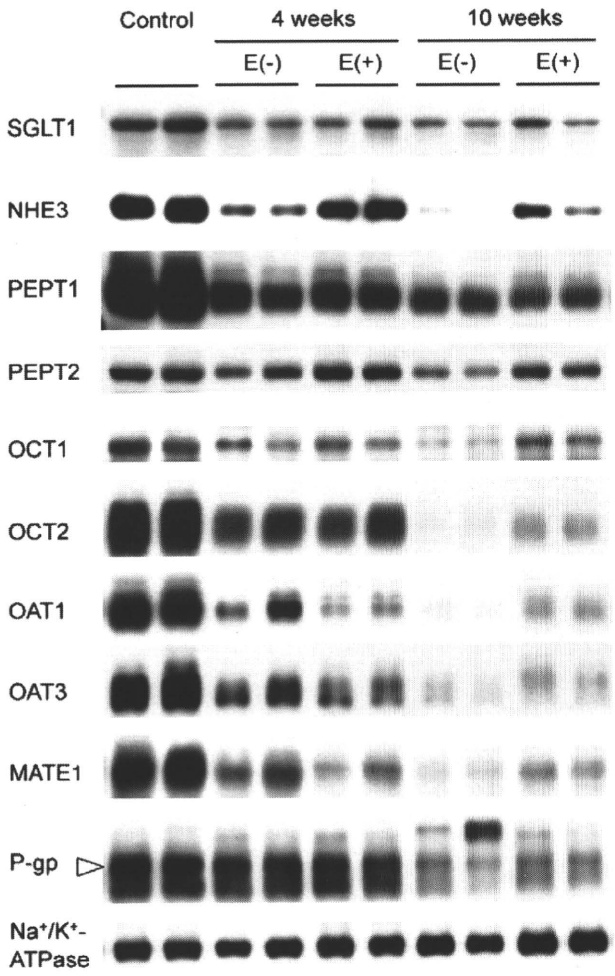

Fig. 8. Expression of proximal tubular transporters in the crude plasma membrane fractions of remnant kidneys. Four weeks and 10 weeks represent groups in which a 14-day subcutaneous administration of everolimus (2 mg/kg/day) or vehicle was initiated at 2 and 8 weeks after surgery, respectively. Antisera specific for each transporter (1:1000–10,000 dilution) were used as primary antibodies. Control, membranes obtained from normal kidney; E(−), Nx rats administered vehicle; E(+), Nx rats administered everolimus.

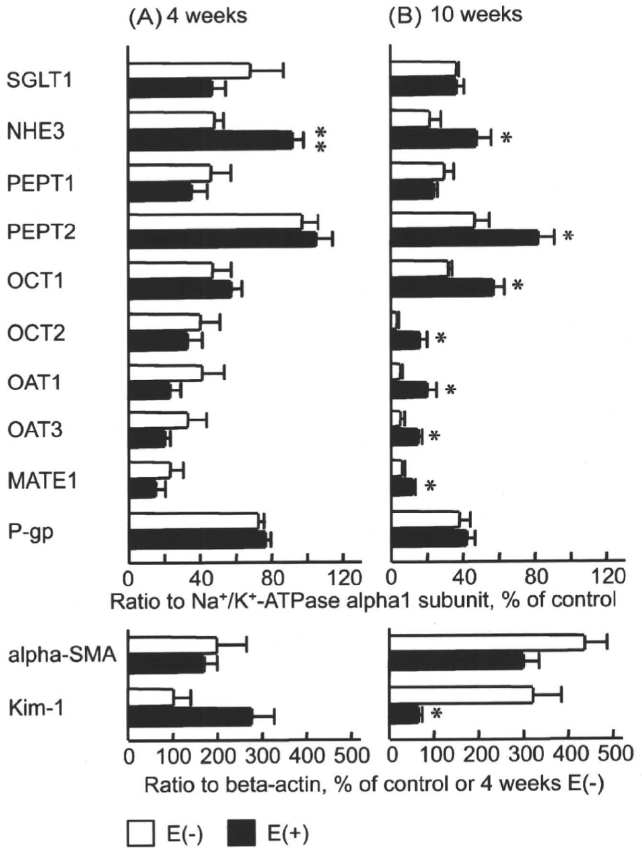

Fig. 9. Effects of everolimus on the protein expression levels of transporters, alpha-SMA and Kim-1. Four weeks (A) and 10 weeks (B) represent groups in which a 14-day subcutaneous administration of everolimus (2 mg/kg/day) or vehicle was initiated at 2 and 8 weeks after surgery, respectively. The densitometric ratio relative to control rat kidneys (for transporters and alpha-SMA) or to the group 4 weeks E(−) (for Kim-1) were shown as the reference. As internal standards, Na^+/K^+-ATPase alpha1 subunit (for transporters) and beta-actin (for alpha-SMA and Kim-1) were used. Values are the mean ± SEM. E(−), 5/6 nephrectomized rats administered vehicle; E(+), 5/6 nephrectomized rats administered everolimus. $^*P < 0.05$, $^{**}P < 0.01$, significantly different from E(−) rats.

in the proximal tubules, and this pharmacological response is at least a part accountable for the decrease in albuminuria.

We previously found that the tubular secretion of ionic drugs such as *para*-aminohippuric acid and cimetidine was markedly decreased in Nx rats, and a down-regulation of organic ion transporters was responsible for these pharmacokinetic changes [3–6]. Interestingly, everolimus recovered the protein expression of these transporters even in the advanced stage of CRF (Fig. 8). Furthermore, it was revealed that the everolimus-treatment restored the expression levels of NHE3 and PEPT2 (Fig. 8), which play roles in maintaining the pH gradient across the luminal membrane [36] and reabsorption of oligopeptides and peptide mimics [37] in the proximal tubules, respectively. In the kidney, numerous membrane transporters play crucial roles as a detoxicating mechanism in the elimination of organic compounds, such as uremic toxin, into urine via tubular secretion [9,38–40]. Therefore, mTOR inhibition by everolimus in CRF is indicated to be able to bring restoration of tubular functions including the reabsorption of albumin and nutrients, homeostasis in the acid–base balance and detoxication by recovering the membrane transporters in the polarized epithelia.

Although Kim-1 has been characterized as a urinary biomarker of acute kidney injury, little information about its role was clarified in progressive renal failure [41]. In the present study, we have first found that the expression of Kim-1 was induced in the proximal tubules with time after nephrectomy (Fig. 6). The expression of Kim-1 is increased in the injured kidney [23] and is predominantly localized to the apical membrane acting as a receptor for the phagocytosis of apoptotic cells by the proximal tubular epithelium itself [42]. In FITC-albumin-administered rat kidneys, the red signal area with Kim-1 antibody was almost independent from the area of green signals for FITC-albumin (Fig. 7G and H). As expected, the red signal area with Kim-1 antibody was decreased with the increase in the condensed green signals for FITC-albumin in response to the administration of everolimus (Figs. 6 and 7). These results suggested that the inhibition of the mTOR pathway recovered the tubular function coinciding with the amelioration of progressive tubular dysfunction and decrease the expression of Kim-1 in CRF proximal tubules.

Tubular atrophy and interstitial fibrosis are the final common steps on the progression of chronic kidney disease [1]. Epithelial-mesenchymal transition (EMT) is considered to have a crucial role in this pathogenesis [43]. In Nx rats, EMT was observed in the remnant kidney, and alpha-SMA was shown to be a marker for EMT [44,45]. On the other hand, it was reported that the activation of